Fluorescence Studies of Dehydroergosterol in Phosphatidylethanolamine/Phosphatidylcholine Bilayers

Kwan Hon Cheng,* Jorma Virtanen,# and Pentti Somerharju§

*Department of Physics, Texas Tech University, Lubbock, Texas 79409; #Department of Radiology, University of California at Irvine, Irvine, California 92697; and §Department of Medical Chemistry, University of Helsinki, Helsinki 00014, Finland

ABSTRACT   Our previous fluorescence study has provided indirect evidence that lipid headgroup components tend to adopt regular, superlattice-like lateral distribution in fluid phosphatidylethanolamine/phosphatidylcholine (PE/PC) bilayers (Cheng et al., 1997, *Biophys. J.* 73:1967–1976). Here we have further studied this intriguing phenomenon by making use of the fluorescence properties of a sterol probe, dehydroergosterol (DHE). Fluorescence emission spectra, fluorescence anisotropy (r), and time-resolved fluorescence intensity decays of DHE in 1-palmitoyl-2-oleoyl-PC (POPC)/1-palmitoyl-2-oleoyl-PE (POPE) mixtures were measured as a function of POPE mole fraction (X_{PE}) at 23°C. Deviations, including dips or kinks, in the ratio of fluorescence peak intensity at 375 nm/fluorescence peak intensity at 390 nm (I_{375}/I_{390}), fluorescence decay lifetime (τ), or rotational correlation time (ρ) of DHE versus PE composition plots were found at $X_{PE} \approx$ 0.10, 0.25, 0.33, 0.65, 0.75, and 0.88. The critical values at $X_{PE} \approx$ 0.33 and 0.65 were consistently observed for all measured parameters. In addition, the locations, but not the depth, of the dips for $X_{PE} < 0.50$ did not vary significantly over 10 days of annealing at 23°C. The observed critical values of X_{PE} coincide (within ±0.03) with some of the critical mole fractions predicted by a headgroup superlattice model proposing that the PE and PC headgroups tend to be regularly distributed in the plane of the bilayer. These results agree favorably with those obtained in our previous fluorescence study using dipyrenylPC and Laurdan probes and thus support the proposition that 1) regular arrangement within a domain exists in fluid PE/PC bilayers, and 2) superlattice formation may play a significant role in controlling the lipid composition of cellular membranes (Virtanen et al., 1998, *Proc. Natl. Acad. Sci. USA.* 95:4964–4969). The present data provide new information on the physical properties of such superlattice domains, i.e., the dielectric environment and rotational motion of membrane sterols appear to change abruptly as the lipid headgroups exhibit regular superlattice-like distributions in fluid bilayers.

INTRODUCTION

A recent study (Cheng et al., 1997) suggested that phospholipid headgroups of fluid binary phosphatidylcholine/phosphatidylethanolamine (PC/PE) membranes may exhibit regular superlattice-like domains at certain critical PE molar fractions. Using noninvasive Fourier transform infrared spectroscopy and steady-state fluorescence measurements based on site-specific fluorescent probes, Laurdan and dipyrenylPC, evidence that 1-palmitoyl-2-oleoyl-PE (POPE) and 1-palmitoyl-2-oleoyl-PC (POPC) molecules adopt superlattice arrangements at several PE mole fractions (X_{PE}), 0.04, 0.11, 0.16, 0.26, 0.33, 0.51, 0.66, 0.75, 0.82, 0.91, and 0.94, has been presented (Cheng et al., 1997). Another study indicated that such superlattice arrangements could also exist in natural membranes, and it was proposed that they might play a crucial role in the compositional regulation of such membranes (Virtanen et al., 1998; Somerharju et al., 1999). Notably, sterols also seem to adopt superlattice-like arrangements in membranes (Chong, 1994; Parasassi et al., 1995; Virtanen et al., 1995). However, more experimental evidence on superlattice formation needs to be

obtained. The effects of superlattice formation on the location and dynamics of membrane components also need to be determined.

In the present study, a small fixed amount of fluorescent sterol, dehydrergosterol (DHE), was incorporated into the binary POPE/POPC mixtures. An extensive study, including both steady-state and time-resolved fluorescence measurements, was performed for $X_{PE} = 0.08–0.92$. The aim of this study was to determine whether these new fluorescent sterol measurements would reveal the presence of critical compositions and whether those compositions would agree with those predicted by the headgroup superlattice model (Virtanen et al., 1998). In addition, the effects of the putative superlattice formation on the location and dynamics of sterols (as reported by DHE) in the membrane were investigated.

MATERIALS AND METHODS

Lipid membrane preparations

Lipids were purchased from Avanti Polar Lipids (Alabaster, AL) and were found to be more than 99% pure, based on thin-layer chromatography analysis. DHE was obtained from Sigma (St. Louis, MO). The stock solutions containing POPC and POPE in varying ratios were mixed in chloroform, and a small amount of DHE (1.0 mol%) was added. The samples were placed in a 42°C water bath, and the solvent was evaporated under a nitrogen stream. Any residual solvent was removed by keeping the samples under vacuum at 42°C for at least 5 h. The dry lipid films were subsequently dispersed in buffer (100 mM NaCl/10 mM *N*-tris-(hydroxymethyl) methyl-2-aminoethanesulfonic acid/2 mM EDTA, pH 7.4) at 35°C and under rigorous vortexing for 15 min. After more than 24 h of incuba-

tion at 4°C, the lipid samples were kept at 35°C for 30 min and then at 4°C. This temperature cycling was repeated at least three times. The samples were kept in the dark at 4°C before any spectroscopic measurements.

Laser-induced fluorescence measurements

Fluorescence spectral measurements were performed on a home-built optical multichannel analyzer equipped with a UV-enhanced proximity focused intensified photodiode array IRY-700S detector (Princeton Instrument, Trenton, NJ), which was attached to a 1/3 m SPEX Minimate 1681 spectrograph (SPEX Industries, Edison, NJ). A Liconix 4240NB cw UV He-Cd laser (Santa Clara, CA) operating at 325 nm was used for excitation. With this instrument, a single fluorescence spectrum was obtained in less than 50 ms with a wavelength resolution of 0.24 nm. Normally 20–50 spectra were accumulated, from which the peak intensity ratio was calculated. Steady-state fluorescence emission anisotropy measurements were performed on an ISS GREG 200 (ISS, Champaign, IL) fluorometer, using an L-format arrangement with excitation at 325 nm and the same He-Cd laser as above. Fluorescence emission was collected through a 380-nm low-cutoff filter.

Fluorescence lifetime measurements were performed on the same ISS GREG 200 fluorometer equipped with digital multifrequency cross-correlation phase and modulation acquisition electronics. The same He-Cd laser was also used for excitation. An excitation polarizer with its transmission axis set at 35° with respect to the vertical was placed in the excitation beam to eliminate the contribution of the rotational diffusion effect of the sample to the measurements (Spencer and Weber, 1970). No polarizer was placed on the emission side. Phase delay and demodulation values of the DHE fluorescence signal were compared with that of a standard solution (*p*-bis[2-(5-phenyloxzaolyl0]benzene (POPOP) in ethanol, fluorescence lifetime = 1.35 ns) and measured at different modulation frequencies ranging from 5 to 200 MHz. All fluorescence measurements were carried out at 23°C. The samples were equilibrated at 23°C for at least 45 min before the measurements.

Fluorescence data analysis

In general, the time-resolved fluorescence intensity decay [$I(t)$] of a fluorescent sample can be expressed by a sum of exponential decays, i.e.,

$$I(t) = \sum_{i}^{n} \alpha_i e^{-t/\tau_i}, \tag{1}$$

where τ_i and α_i are the fluorescence decay lifetime and the preexponential factor, or mole fraction, of the *i*th resolved fluorescence component, and *n* is the total number of components. In the frequency-domain measurements, the values of τ_i and α_i can be recovered using a nonlinear least-squares procedure. The average fluorescence decay lifetime $\langle\tau\rangle$ can be calculated from the equation given by

$$\langle\tau\rangle = \sum_{i}^{n} f_i \tau_i, \tag{2}$$

where f_i is the intensity fraction of the *i*th component and can be further expressed as

$$f_i = \alpha_i \tau_i \Big/ \sum_{i}^{n} \alpha_i \tau_i. \tag{3}$$

The rotational correlation time ρ, a parameter inversely proportional to the average rate of rotation, of the fluorescent probe can be obtained from the measured average lifetime $\langle\tau\rangle$ and steady-state anisotropy *r*, using the Perrin equation (Perrin, 1936),

$$\rho = \frac{\langle\tau\rangle}{(r_0/r - 1)}, \tag{4}$$

where r_o is the limiting anisotropy and has been estimated to be 0.37 for DHE in lipid membranes (Chong and Thompson, 1986).

Lipid headgroup superlattice model

Assuming that the phospholipid headgroups are hexagonally (HX) or rectangularly (R) arranged, the critical PE mole fractions, $X_{HE,PE}$ or $X_{R,PE}$, respectively, for a binary system of PE/PC with mole fraction of PE (X_{PE}) are obtained from the equations

$$X_{HX,PE} = \frac{1}{a^2 + ab + b^2}$$

or

$$X_{R,PE} = \frac{1}{ab + b^2} \quad \text{for } X_{PE} < 0.5 \tag{5}$$

and

$$X_{HX,PE} = 1 - \frac{1}{a^2 + ab + b^2}$$

or

$$X_{R,PE} = 1 - \frac{1}{ab + b^2} \quad \text{for } X_{PE} > 0.5, \tag{6}$$

where *a* and *b* refer to the distance between two proximal guest headgroups, given in lattice sites along the principal lattice axes (Cheng et al., 1997; Virtanen et al., 1998). The critical mole fractions thus distribute symmetrically around $X_{PE} = 0.5$. Some representative critical mole fractions and their lattice constants (*a, b*) are shown in Table 1.

RESULTS

Steady-state fluorescence measurements (intensity ratio from emission spectra and emission anisotropy) of DHE in POPE/POPC mixtures of varying PE contents ($X_{PE} = 0.08$–0.92) were performed at 23°C. The separation between two successive PE mole fractions is 0.005 for all POPE/POPC samples. Because it is impractical to cover the entire composition region in a single experiment, three sets of samples covering the low-PE ($X_{PE} = 0.08$–0.40), mid-PE ($X_{PE} = 0.40$–0.60), and high-PE ($X_{PE} = 0.60$–0.92) regions were prepared. In each case, three parallel (or independently prepared) samples were prepared and averaged. In addition, the data were smoothed by using a three-point running average. Time-resolved fluorescence decay measurements of DHE in POPE/POPC mixtures of varying PE contents were also performed. For each sample, more than 20 min was needed to complete one fluorescence decay measurement. Therefore, the PE mole fractions were less closely spaced (typically 0.01–0.02) than in the case of steady-state measurements. After equilibration of the samples at the measurement temperature of 23°C for at least 45 min, the

TABLE 1 Comparison of critical mole fractions X_{PE} from measured DHE fluorescence parameters (intensity peak ratio, steady-state anisotropy) and calculated DHE fluorescence and rotation parameters ($\langle \tau \rangle$ and ρ) with $X_{HX,PE}$ and $X_{R,PE}$ values predicted by the HGSL model for PE/PC mixtures

$X_{HX,PE}$ (a, b)	$X_{R,PE}$ (a, b)	Intensity peak ratio	Anisotropy	$\langle \tau \rangle$ (ns)	ρ (ns)
0.111 (3, 0)	0.111 (0, 3)		0.10[d]	0.11[d]	0.11[d]
	0.125 (2, 2)				
0.143 (2, 1)					
	0.167 (5, 1)	0.16[d]			
	0.200 (4, 1)				
0.250 (2, 0)	0.250 (3, 1)	0.25[d]		0.22–0.25[d]	0.22–0.25[d]
0.333 (1, 1)	0.333 (3, 1)	0.35[d]	0.33[d]	0.32–0.36[d]	0.32–0.36[d]
	0.500 (1, 1)	0.43–0.50[k]	0.45–0.50[d]		0.46–0.53[k]
0.667 (2, 1)	0.667 (2, 1)	0.65[k]	0.70[k]	0.62–0.65[d]	0.62–65[d]
0.750 (2, 0)	0.750 (3, 1)	0.75[k]	0.77[k]		
	0.800 (4, 1)				
	0.833 (5, 1)				
0.857 (2, 1)					
	0.875 (2, 2)				
0.889 (0, 3)	0.889 (0, 3)	0.88[k]	0.88[k]		0.88[d]

The lattice coordinates (a, b) are also given (see Eqs. 5 and 6). Critical mole fractions are determined by the observed major dips and kinks in the DHE parameter versus PE composition plots and are denoted by superscripts d and k, respectively.

steady-state and time-resolved fluorescence measurements were carried out within 2–3 h.

Low-PE region (X_{PE} = 0.08–0.40)

Steady-state fluorescence measurements

Two major fluorescence peaks, at 375 and 390 nm, and a small shoulder at 418 nm were found in all DHE spectra. Fig. 1 *A* shows a few representative spectra of DHE for X_{PE} = 0.29, 0.31, 0.33, 0.35, and 0.37. The spectra were normalized at the 375-nm major peak. As the PE content increased from 0.29 to 0.33, the intensity of the peak at 390 nm and that of the shoulder at 418 nm increased steadily with the PE composition. However, as the PE content increased further from 0.33 to 0.37, the intensities at 390 and 418 nm began to drop. The DHE spectrum for X_{PE} = 0.37 was found to be almost identical to that for X_{PE} = 0.31. Fig. 1 *B* shows the difference spectra, obtained by subtracting the normalized spectra for X_{PE} = 0.31, 0.33, 0.35, and 0.37 from the normalized spectrum for X_{PE} = 0.29. The rather subtle changes in the intensities at 390 and 418 nm are clearly demonstrated in these difference spectra. Although the absolute intensity of fluorescence varied among samples, the changes in the spectral features were found consistently at X_{PE} ≈ 0.33. Because of the well-resolved fluorescence peaks at 375 and 390 nm in all samples, a useful spectral parameter, i.e., the fluorescence intensity at 375 nm divided by the fluorescence intensity at 390 nm (I_{375}/I_{390}), was calculated from each spectrum measured for DHE in POPE/POPC mixtures. Fig. 2 *B* shows the composition-dependent changes of I_{375}/I_{390} in the low-PE region. Apparent dips at X_{PE} ≈ 0.16, 0.25, and 0.35 were observed. In addition, a deviation at X_{PE} ≈ 0.11 may be present but is defined by only a single low data point and thus considered uncertain. Fig. 2 *A* shows the composition-dependent

changes of the average fluorescence intensity at 375 nm. Dips at X_{PE} ≈ 0.16, 0.25, and 0.35 were also observed. Steady-state fluorescence anisotropy measurements revealed a prominent dip at X_{PE} ≈ 0.33 and, possibly, a small dip or kink at X_{PE} ≈ 0.10 and a broad dip at X_{PE} ≈ 0.17 (Fig. 2 *C*).

Time-resolved fluorescence measurements

Fig. 3 shows the representative frequency domain data, phase delay, and modulation ratio for DHE when X_{PE} = 0.29, 0.33, or 0.37. Both monoexponential and biexponential decay functions, corresponding to n = 1 and 2 in Eq. 1, respectively, were fitted to the frequency-domain data. Table 2 shows the recovered fluorescence lifetime parameters based on a nonlinear regression analysis. The values of the reduced χ^2 of the biexponential fits were found to be smaller than those of the monoexponential fits for all PE contents. This observation agrees with the fact that the theoretical biexponential curves fit the frequency domain data much better than do the theoretical monoexponential curves as shown in Fig. 3 for all PE contents. No significant improvements in the values of reduced χ^2 were found when more complicated decay functions, like triexponential or continuous distribution (results not shown), were used. The values of the average lifetimes $\langle \tau \rangle$ of DHE were also calculated as given by Eq. 3. The value of $\langle \tau \rangle$ for X_{PE} = 0.33 was found to be lower than that for X_{PE} = 0.29 or 0.37. A similar trend was found for the single fluorescence lifetimes obtained from the monoexponential fits and is shown in Table 2.

Fig. 4 summarizes the fluorescence lifetime data of DHE in the low-PE region. A dip at X_{PE} ≈ 0.22 is indicated for the long τ and, perhaps, for the short τ, as shown in Fig. 4 *A*. For the average fluorescence lifetime $\langle \tau \rangle$, a sharp kink at
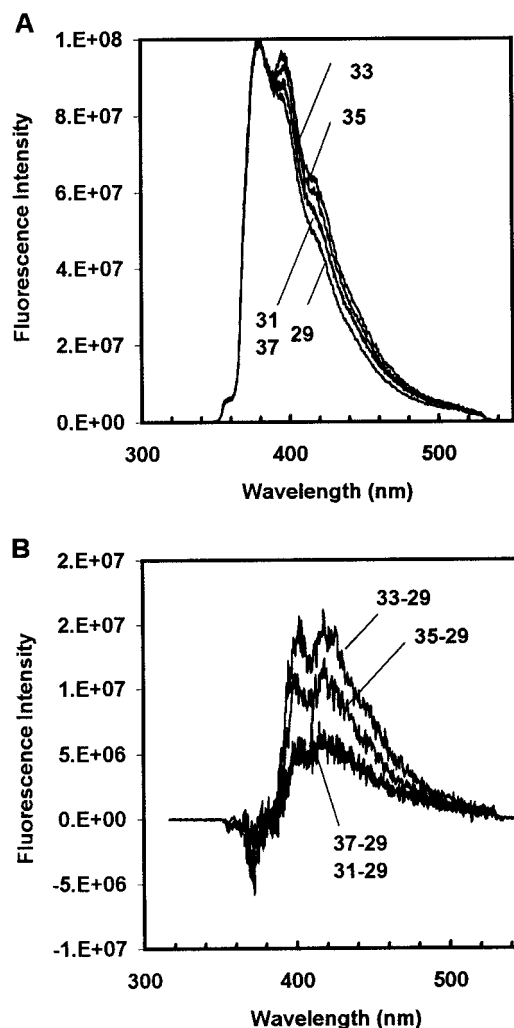
FIGURE 1 Normalized fluorescence spectra of DHE in POPE/POPC mixtures for 29, 31, 33, 35, and 37 mol % PE at 23°C (A), and their corresponding difference spectra (B) obtained by subtracting the normalized spectra for 31, 33, 35, and 37 mol% PE from the normalized spectrum for 29 mol% PE. Excitation was set at 325 nm.

$X_{PE} \approx 0.11$ and two broad dips at $X_{PE} \approx 0.22$–0.25 and 0.32–0.36 seem to be present (Fig. 4 C). Based on the Perrin equation (Eq. 4), the rotational correlation time ρ was calculated from the values of $\langle \tau \rangle$ and steady-state anisotropy as given by Eq. 4. Fig. 5 A shows the composition-dependent changes of ρ as a function of PE content in the low-PE region. These data are compatible with but do not clearly show the existence of a sharp dip at $X_{PE} \approx 0.11$ and broad dips at $X_{PE} \approx 0.22$–0.25 and 0.32–0.36.

Mid-PE region ($X_{PE} = 0.40$–0.60)

Steady-state fluorescence measurements

Fig. 6 B shows the composition dependency of I_{375}/I_{390} in the mid-PE region. No clear dips can be observed, but a deviation at $X_{PE} \approx 0.43$–0.50 seems to be present. The fluorescence intensities at 375 nm are shown in Fig. 6 A. No
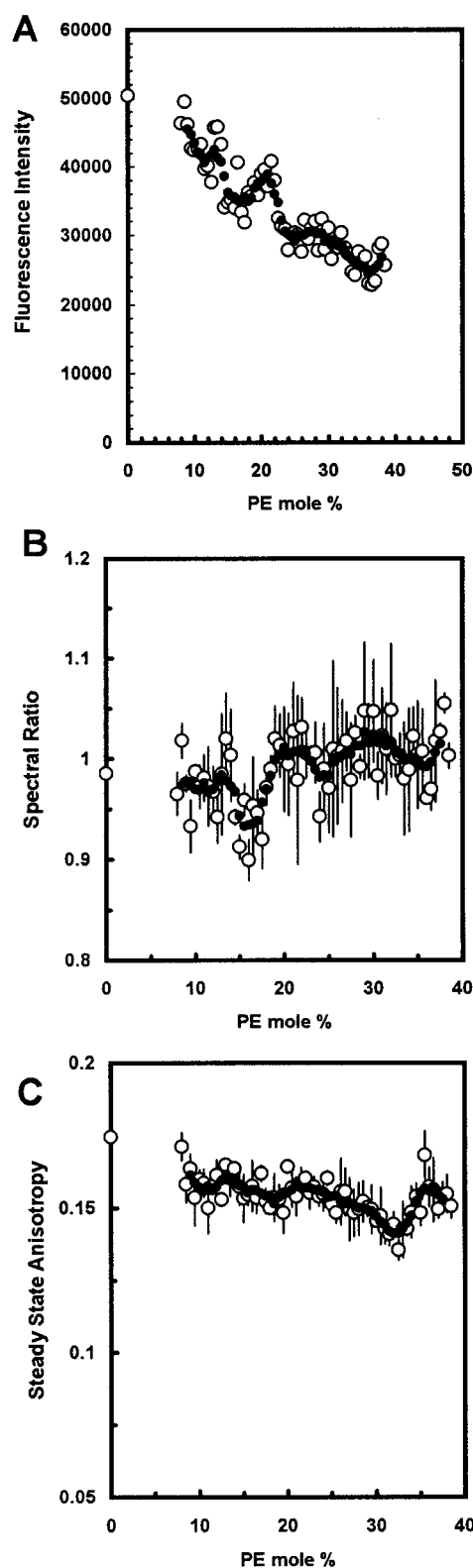

FIGURE 2 Steady-state fluorescence parameters, fluorescence intensity at 375 nm (A), spectral ratio, i.e., peak intensity at 375 nm/peak intensity at 390 nm (I_{375}/I_{390}) (B), and anisotropy (C), of DHE in POPE/POPC mixtures at 23°C as a function of PE content in the low-PE region (8–40 mol% PE). Excitation was set at 325 nm. Each point represents an average from measurements of three independently prepared samples of identical composition. Three-point running averages (●) of the data points are also shown. Bars indicate the standard deviations of measurements.
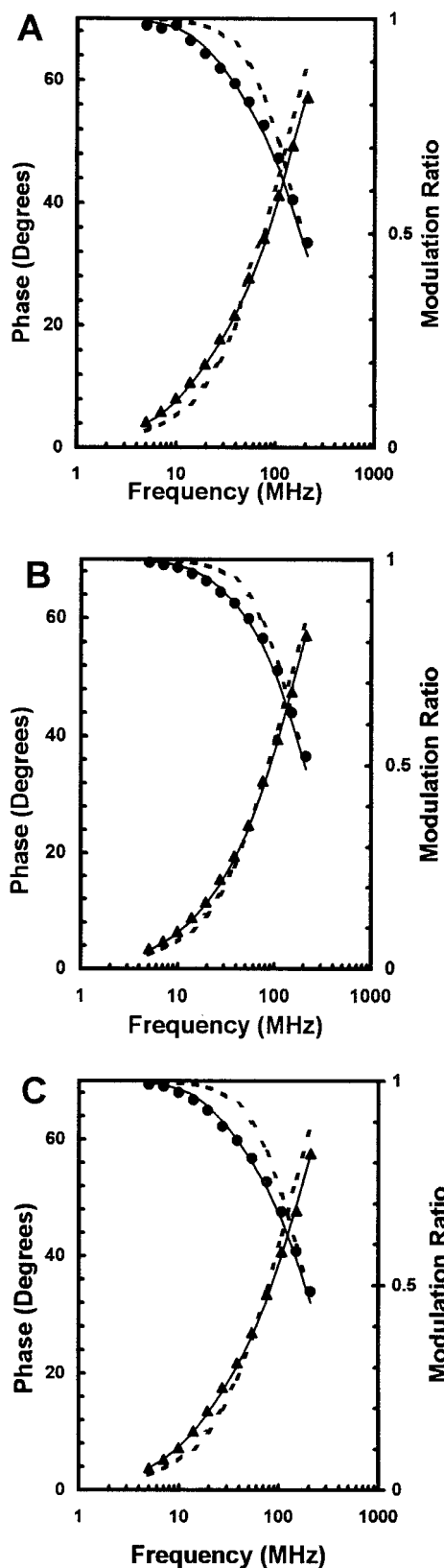
FIGURE 3 Representative frequency domain fluorescence decay data, phase delay (▲), and modulation ratio (●) of DHE in POPE/POPC mixtures for 29 (*A*), 33 (*B*), and 37 (*C*) mol% PE at 23°C. A monoexponential (– – –) or biexponential (——) decay function was fitted to the data points. The corresponding fitted fluorescence decay parameters are also shown in Table 2.

significant deviations were observed. The fluorescence anisotropy measurement supports a deviation at $X_{PE} \approx 0.45$–0.50, as shown in Fig. 6 *C*.

Time-resolved fluorescence measurements

Fig. 7 summarizes the fluorescence lifetime data of DHE in this mid-PE region. No significant changes were observed for the values of the resolved long and short lifetimes and the short lifetime fractions (Fig. 7, *A* and *B*). Again, no significant deviations were found for the values of $\langle \tau \rangle$ as shown in Fig. 7 *C*. Fig. 5 *B* shows the composition-dependent changes of ρ as a function of PE content in the mid-PE region. Here a broad deviation at $X_{PE} \approx 0.46$–0.53 was observed.

High-PE region ($X_{PE} = 0.60$–0.92)

Steady-state fluorescence measurements

Fig. 8 *B* shows the composition dependency of I_{375}/I_{390} in the high-PE region. An obvious kink at $X_{PE} \approx 0.75$ and, possibly, smaller kinks at $X_{PE} \approx 0.65$ and 0.88 are present. The fluorescence intensities are shown in Fig. 8 *A*. A kink at $X_{PE} \approx 0.75$ and, possibly, a dip at $X_{PE} \approx 0.65$ are present. The anisotropy data are rather noisy but are compatible with kinks being present at $X_{PE} \approx 0.67$–0.70 and 0.77–0.80 and close to 0.88 (Fig. 8 *C*).

Time-resolved fluorescence measurements

Fig. 9 summarizes the fluorescence lifetime data of DHE in the high-PE region. A broad dip at $X_{PE} \approx 0.63$–0.65 was observed in the values of long τ as shown in Fig. 9 *A*. The fraction of short τ indicates a broad peak at $X_{PE} \approx 0.65$–0.70 (Fig. 9 *B*). The average lifetime $\langle \tau \rangle$ is compatible with a broad dip at $X_{PE} \approx 0.62$–0.65 (Fig. 9 *C*). Fig. 5 *C* shows the composition-dependent changes of ρ as a function of PE content in the high-PE region. A dip close to $X_{PE} \approx 0.65$ and a possible deviation close to $X_{PE} \approx 0.80$ were found.

Stability of dips

To determine the stability of the observed dips, low-PE samples were kept at 23°C, i.e., the temperature of fluorescence measurements in this study, for up to 10 days. Measurements were made on the first, third, fourth, sixth, eighth, and tenth days after preparation and temperature cycling (see Materials and Methods). The locations and depth of the DHE spectral ratio and anisotropy dips were determined. The depth of a dip is defined as (max − min)/max × 100, where max and min are the local maximum and minimum within a given local region of X_{PE}, i.e., 0.09–0.14, 0.14–0.21, 0.21–0.30, or 0.30–0.39. As shown in Fig. 10 *A*, the spectral ratio dips at $X_{PE} \approx 0.11$, 0.17, 0.24, and 0.34 were present and remained invariant within ±0.02, and the depth

TABLE 2 Fluorescence decay parameters of DHE in PE/PC mixtures

X_{PE}	τ_1 (ns)	Biexponential fit					Monoexponential fit	
		α_1	τ_2 (ns)	$\langle\tau\rangle$ (ns)	χ^2		τ (ns)	χ^2
0.29	1.14 ± 0.03	0.94 ± 0.05	5.64 ± 0.63	2.23 ± 0.28	17.5		1.47 ± 0.15	247.6
0.33	1.13 ± 0.03	0.96 ± 0.04	5.43 ± 0.86	1.77 ± 0.26	11.1		1.31 ± 0.08	98.6
0.37	1.11 ± 0.01	0.93 ± 0.04	5.22 ± 0.47	2.13 ± 0.22	12.0		1.43 ± 0.14	223.5

of all these dips became stabilized at 2% after the third day of annealing at 23°C.

Similar results were obtained for the anisotropy dips at $X_{PE} \approx 0.10$, 0.16, and 0.32 (Fig. 11). However, the depth of the anisotropy dips remained at the level of 10% for the two small dips at $X_{PE} \approx 0.10$ and 0.16, but increased to 30% for the prominent dip at $X_{PE} \approx 0.32$ after 10 days of annealing.

DISCUSSION

The present study supports our previous findings by showing significant dips/deviations at certain critical compositions predicted by a headgroup superlattice model (Cheng et al., 1997). As was noted in the Introduction, the existence of such a critical composition could be intimately involved in the regulation of lipid compositions of biological membranes (Virtanen et al., 1998; Somerharju et al., 1999). Table 1 provides a summary of the observed composition-dependent changes in the measured DHE fluorescence parameters (steady-state intensity peak ratio, steady-state anisotropy) and the calculated DHE fluorescence and rotational parameter (average fluorescence lifetime $\langle\tau\rangle$ and rotational correlation time ρ). The changes are categorized based on the appearances of kinks or dips from the above DHE parameters versus PE composition plots for the low-PE, mid-PE, and high-PE regions. Our data points represent averages of fluorescence measurements from three independently prepared samples. Notably, our fluorescence measurement using dipyrenyl probes (results not shown) indicated that the T_m decreases from 26°C at $X_{PE} = 1.00$ to ~21°C at $X_{PE} = 0.95$. Therefore the POPE/POPC bilayers are essentially in the fluid state at 23°C for $X_{PE} = 0.92$, which is the maximum PE content of this study.

The major dips for $X_{PE} < 0.50$ appeared reproducibly at certain compositions upon repeated measurements during a 10-day postpreparation period. This is important because positions of the dips should not depend on time if they indeed mark the critical compositions predicted by the superlattice model (Cheng et al., 1997; Virtanen et al., 1998; Somerharju et al., 1999). On the other hand, the depth of many dips appeared to change with time. We believe that the magnitude, or depth, of a dip depends on the relative amount of regular distributed domains and the coexisting nonregular domains. In addition, there may have been a significant nonequilibrium component immediately after the sample preparation, and the formation of certain superlattice domains may require stability or at least metastability.

Dehydroergosterol (DHE), a fluorescent sterol probe, has been used extensively when the structure and function of lipid membranes have been studied (Schroeder, 1984; Chong and Thompson, 1986; Bar et al., 1989; Kao et al., 1990; Liu et al., 1997; Loura and Prieto, 1997). The structure of DHE is similar to that of cholesterol (Schroeder, 1984). The fluorescence intensity, spectral ratio, and lifetime of DHE are useful indicators of the dielectric constant of the microenvironment of membrane sterols in bilayers (Schroeder et al., 1987; Liu et al., 1997). By combining the fluorescence lifetime and steady-state fluorescence anisotropy data, the average rotational correlation time, which is inversely related to the rotational rate, of DHE in the membranes can also be estimated (Liu et al., 1997). In a recent study of sterol/PC mixtures (Liu et al., 1997), the above physical parameters of DHE exhibited dips/peaks at several mole fractions of sterols. Those mole fractions agree with the critical mole fractions predicted by the acyl chain/sterol superlattice model (Chong, 1994; Virtanen et al., 1995; Liu et al., 1997).

The steady-state fluorescence intensity ratio (I_{375}/I_{390}) and the fluorescence decay lifetime of DHE are useful parameters for the study of the quenching properties of fluorescent sterols in membranes. Quenching of DHE fluorescence is related to with the distribution of DHE within the membrane during its fluorescence lifetime (around a few nanoseconds). Spectral features of DHE in media of different polarities and lipid membranes have been studied extensively (Schroeder, 1984; Loura and Prieto, 1997). In an aqueous medium, DHE has two major fluorescence peaks at 402 and 426 nm. However, when DHE is in a nonpolar medium or in lipid membranes, those peaks shift to 375 and 390 nm. In this study, normalized fluorescence and difference spectra (Fig. 1) of DHE revealed only two major peaks at 375 and 390 nm for all PE contents. The lack of 402-nm and 426-nm peaks indicated that essentially all DHE molecules are located within the membranes. The use of an intensified multichannel optical detection system in this study allowed us to acquire laser-induced fluorescence emission spectra of DHE in PE/PC membranes with reasonably good sensitivity and spectral resolution.

In general, intensity ratio measurements provide an accurate way of studying subtle spectral changes and require no absolute intensity determinations. Near the critical mole fractions, e.g., $X_{PE} \approx 0.33$, a decrease in I_{375}/I_{390} or an increase in the relative fluorescence intensity at the longer wavelength may be related to an increase in the dielectric constant of the microenvironment of DHE. This is sup-
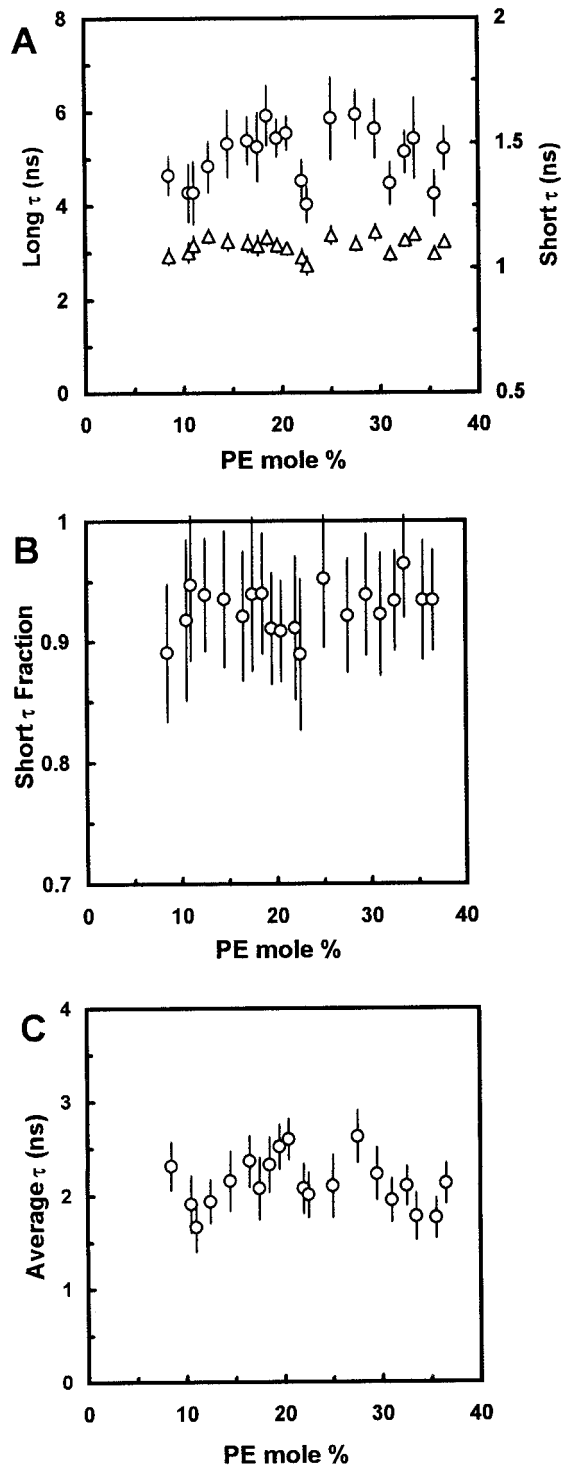
FIGURE 4   Fitted fluorescence decay parameters, long τ ($\bigcirc$) and short τ ($\triangle$) (A), mole fraction of short τ (B), and average τ (C), of DHE in POPE/POPC mixtures at 23°C as a function of PE content in the low-PE region (8–40 mol% PE). Bars indicate the standard deviations of measurements.
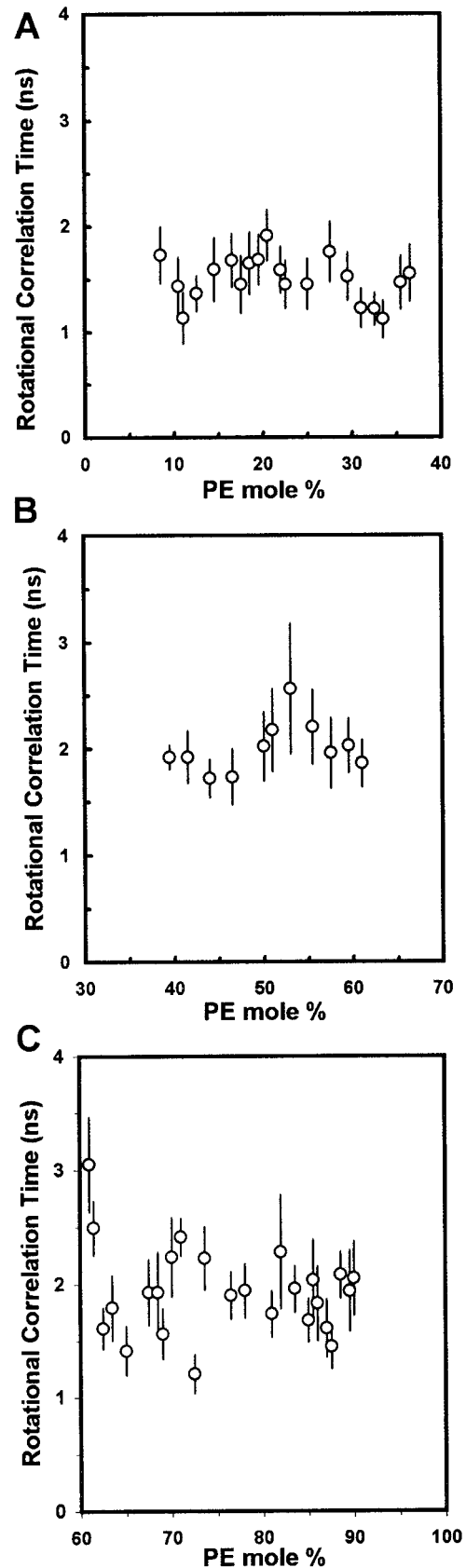

FIGURE 5   Calculated rotational correlation time of DHE in POPE/POPC mixtures at 23°C as a function of PE content in the low-PE region (8–40 mol% PE) (A), mid-PE region (40–60 mol% PE) (B), and high-PE region (60–92 mol% PE) (C). Bars indicate the standard deviations of measurements.
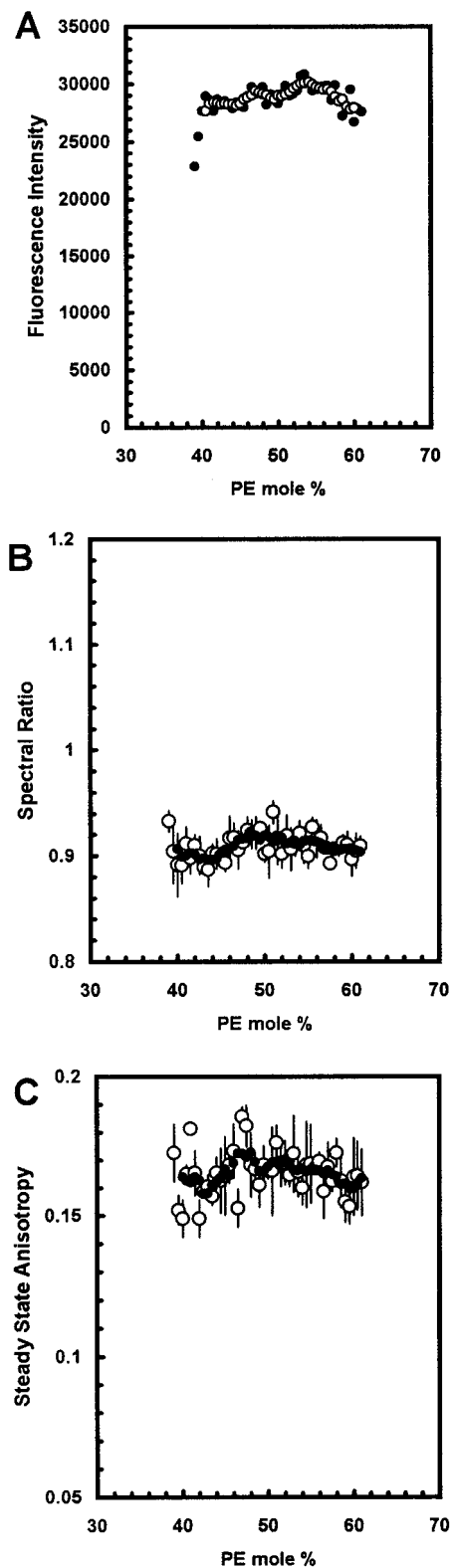
ported by the time-resolved fluorescence decay measurements in which a decrease in $\langle\tau\rangle$ was observed at the mole fractions where dips in I_{375}/I_{390} were found. In addition, fluorescence intensity of the major peak at 375 nm also

FIGURE 6   Steady-state fluorescence parameters, fluorescence intensity at 375 nm (*A*), spectral ratio, peak intensity at 375 nm/peak intensity at 390 nm (I_{375}/I_{390}) (*B*), and anisotropy (*C*), of DHE in POPE/POPC mixtures at 23°C as a function of PE content in the mid-PE region (40–60 mol% PE). Each point represents an average from measurements of three independently prepared samples of identical composition. Three-point running averages (●) of the data points are also shown. Bars indicate the standard deviations of measurements.
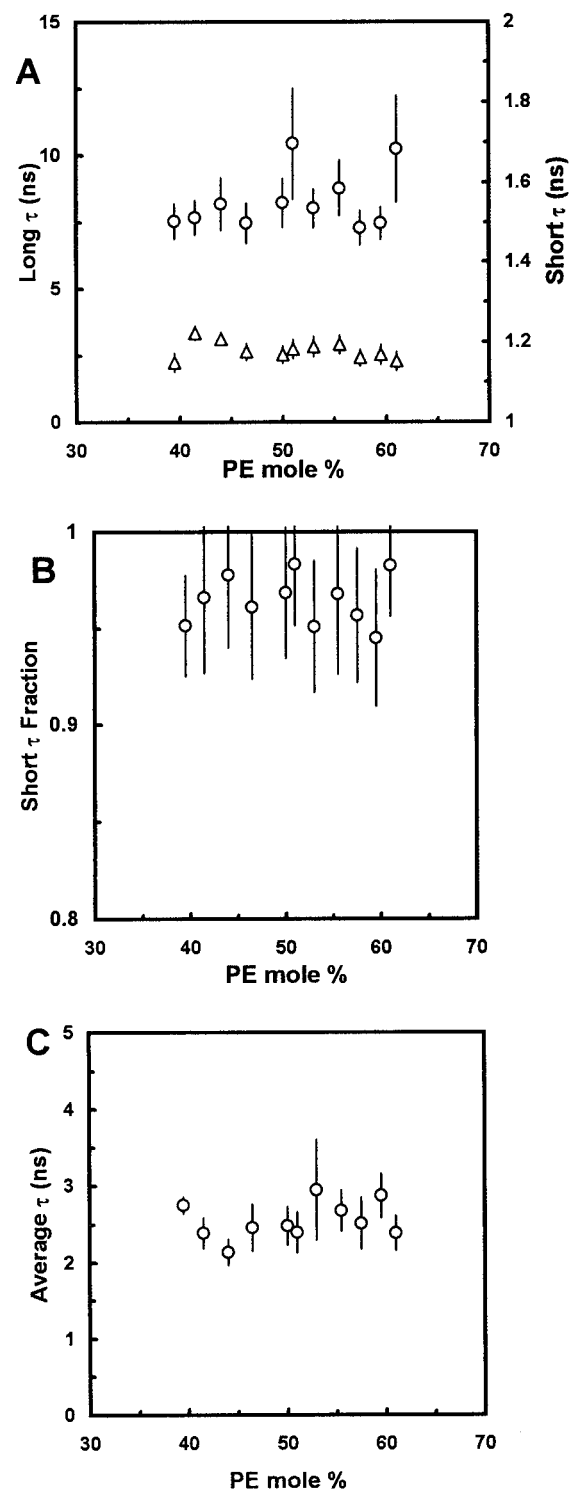
FIGURE 7   Fitted fluorescence decay parameters, long τ (○) and short τ (△) (*A*), mole fraction of short τ (*B*) and average τ (*C*), of DHE in POPE/POPC mixtures at 23°C as a function of PE content in the mid-PE region (40–60 mol% PE). Bars indicate the standard deviations of measurements.

showed a minimum at those critical fractions (Figs. 2 *A*, 6 *A*, and 8 *A*). A previous study (Chong and Thompson, 1986) focusing on acrylamide quenching kinetics of DHE in membranes indicated that the decrease in DHE intensity and
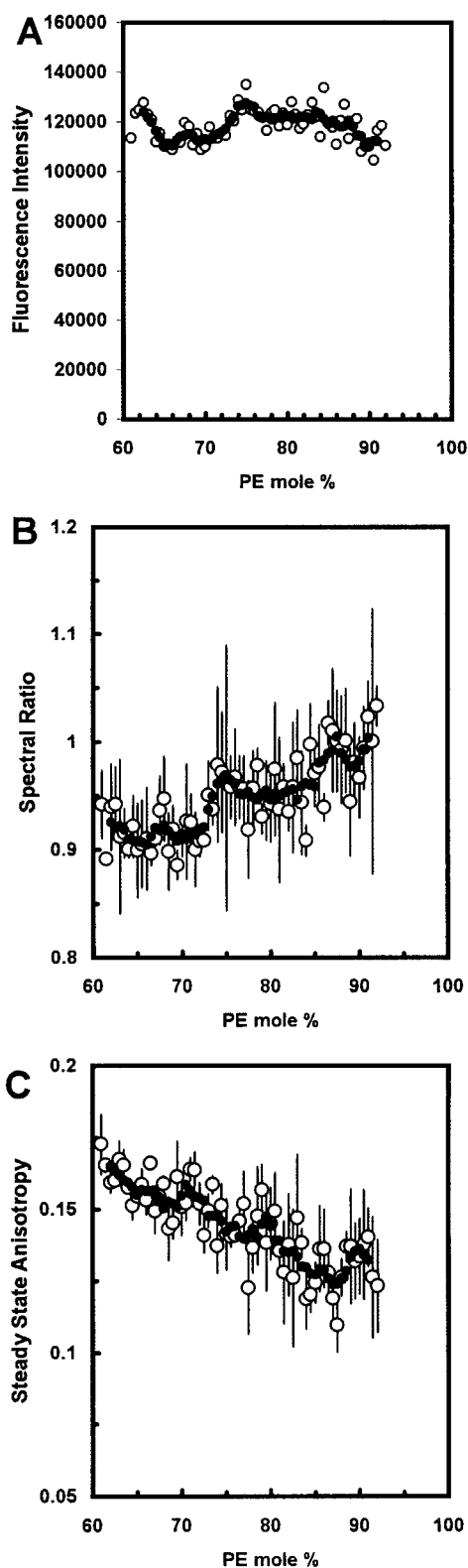
FIGURE 8   Steady-state fluorescence parameters, fluorescence intensity at 375 nm (A), spectral ratio, peak intensity at 375 nm/peak intensity at 390 nm (I_{375}/I_{390}) (B), and anisotropy (C), of DHE in POPE/POPC mixtures at 23°C as a function of PE content in the high-PE region (60–92 mol% PE). Excitation was set at 325 nm. Each point represents an average from measurements of three independently prepared samples of identical composition. Three-point running averages (●) of the data points are also shown. Bars indicate the standard deviations of measurements.
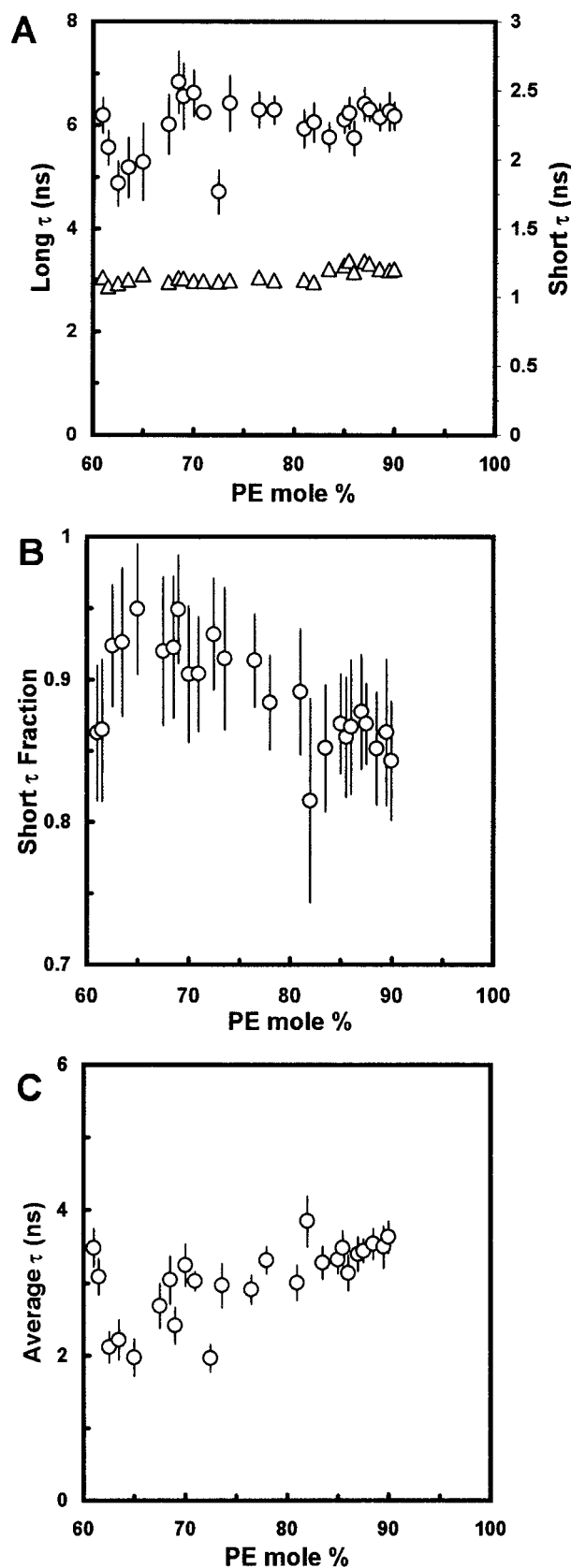

FIGURE 9   Fitted fluorescence decay parameters, long τ (○) and short τ (△) (A), mole fraction of short τ (B), and average τ (C), of DHE in POPE/POPC mixtures at 23°C as a function of PE content in the high-PE region (60–92 mol% PE). Bars indicate the standard deviations of measurements.
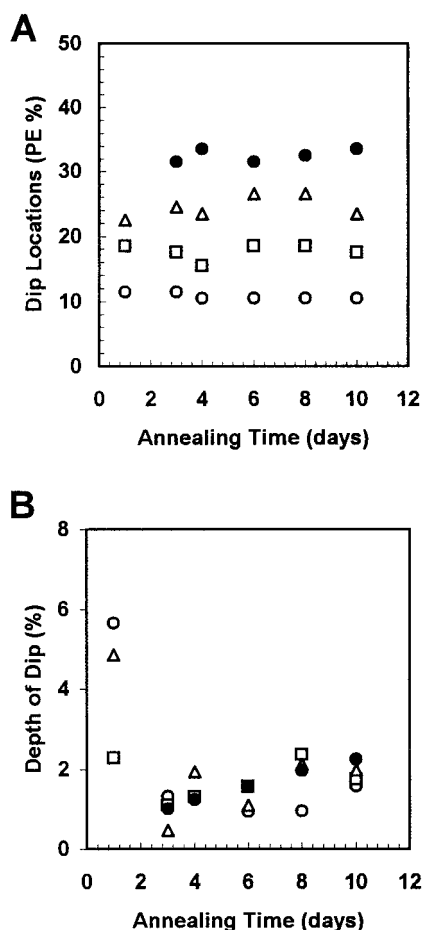
FIGURE 10   Locations (*A*) and depth (*B*) of DHE spectral ratio dips as a function of annealing time at 23°C in the local regions of 9–14 (○), 14–21 (□), 21–30 (△), and 30–39 (●) mol% PE.

FIGURE 11   Locations (*A*) and depth (*B*) of DHE anisotropy dips as a function of annealing time at 23°C in the local regions of 9–14 (○), 14–21 (□), and 30–39 (△) mol% PE.

lifetime can be mainly attributed to an increase in the dielectric constant of the DHE environment in lipid membranes. Other factors may also contribute to the changes in intensity, spectral ratio, or lifetimes. We believe that subtle changes in the dielectric environment of DHE are the major contributions to the observed deviations in I_{375}/I_{390} and $\langle\tau\rangle$. The observations of dips for both I_{375}/I_{390} and $\langle\tau\rangle$ at $X_{PE} \approx$ 0.25, 0.35, and 0.65 lead us to suggest that the dielectric constant of the environment of DHE increases when the host PE/PC membranes adopt regular distributions at the predicted critical mole fractions ($X_{PE} = 0.25$, 0.33, and 0.67).

Usually, the deviations in the I_{375}/I_{390} and $\langle\tau\rangle$ plots, i.e., at $X_{PE} \approx 0.25$ and 0.35, are more obvious in the low-PE region than those in the high-PE region, e.g., $X_{PE} \approx 0.67$. Some (e.g., that at $X_{PE} \approx 0.73$ in Fig. 10 *C*) are defined by only a single composition point and may thus not be taken as an indication of the presence of critical PE composition (e.g., at $X_{PE} = 0.75$), as predicted by the headgroup superlattice model (Virtanen et al., 1998). However, a clear kink in I_{375}/I_{390} at $X_{PE} \approx 0.73$ was found (Fig. 9 *A*). Unfortunately, the spectral ratio is not as straightforward an indicator in revealing the environment of DHE as $\langle\tau\rangle$. Based on
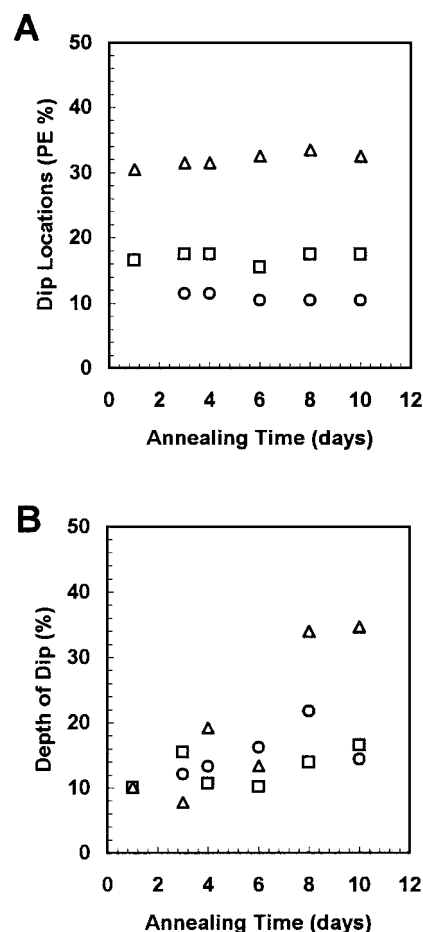
the I_{375}/I_{390} and $\langle\tau\rangle$ data, we propose that membrane sterols, as reported by DHE, are sensing a more polar environment in the superlattice domains as compared to the random domains, within the nanosecond time average. In a recent study on sterol/PC membranes (Liu et al., 1997), a decrease in the lifetime and intensity of DHE was found at several compositions that agreed with the critical compositions predicted by the acyl chain/sterol superlattice model (Liu et al., 1997).

Steady-state fluorescence anisotropy (*r*) measurements provide a qualitative parameter for both the rotational motion and fluorescence decay rate of DHE in the membranes (Perrin, 1936; Chong and Thompson, 1986; Liu et al., 1997). Dips and kinks in the *r* versus composition plots were found at several predicted critical PE mole fractions. Similar to I_{375}/I_{390} and $\langle\tau\rangle$, most of those critical mole fractions, e.g., $X_{PE} \approx 0.10$, 0.33, 0.70, 0.77, and 0.88, were near (±0.03) the mole fractions predicted by the headgroup superlattice model. By using the calculated $\langle\tau\rangle$ data, information on the rotational behavior of DHE can be extracted from *r* based on a simple model (Perrin, 1936). The calculated rotational correlation time ρ is inversely proportional to the average rotational rate of DHE in the membranes.

Dips in the values of ρ for $X_{PE} \approx 0.11$, 0.22, 0.33, 0.50, 0.65, and 0.87 were observed, suggesting that DHE rotates faster in PE/PC membranes at these PE mole fractions, which are close to the critical mole fractions predicted by the headgroup superlattice model, i.e., $X_{PE} = 0.11$, 0.25, 0.33, 0.50, 0.67, and 0.86 (Virtanen et al., 1998). In most cases, the dips in the calculated ρ and those in the calculated $\langle \tau \rangle$ occurred at PE mole fractions close to these predicted ones (see Table 1). However, some of the kinks and dips revealed by steady-state parameters, e.g., $X_{PE} \approx 0.16$ for I_{375}/I_{390} and $X_{PE} \approx 0.17$ and 0.49 for r, were not found in the calculated parameters, $\langle \tau \rangle$ and ρ. These discrepancies may be related to the fact that the calculated parameters are less accurate than or less sensitive to the subtle structural changes in the bilayer structure than the directly measured steady-state parameters. Moreover, the observed changes in some of the measured steady-state parameters may be associated with factors other than the average fluorescence lifetimes or rotational flexibility of DHE. Again, the observed changes in the values of either r or ρ in the low-PE region are much better defined than those in the high-PE region.

Theoretically, the critical mole fractions distribute uniformly around $X_{PE} = 0.5$ (Cheng et al., 1997; Virtanen et al., 1998). In other words, for each critical mole fraction $X_{HX,PE}$ or $X_{R,PE}$ in the low-PE region, there is a critical concentration at $1 - X_{HX,PE}$ or $1 - X_{R,PE}$ in the high-PE region. PE is the guest molecule, whereas PC is the host molecule in the low-PE region. The roles are interchanged, i.e., PE becomes host and PC becomes guest, in the high-PE region. This symmetry of critical compositions appears to be found in our fluorescence measurements, particularly for the detection of the concentration pair at $X_{PE} \approx 0.35$ and 0.65. The difference in the intensities of the composition deviations, i.e., dips and kinks, in the low-PE and high-PE regions could be associated with the two different headgroups participating in the superlattice formation as guest or host. More theoretical and experimental investigations are required to study this issue.

The fluorescence decay analysis may provide new information about the heterogeneity of the DHE environment in membranes. The fluorescence decay of DHE is known to be complex in lipid bilayers, especially in binary ones (Liu et al., 1997). Heterogeneous decay was also observed in the present PE/PC system. The complex decay may be related to the intrinsically heterogeneous environment of any lipid membrane. It is interesting to note that close to some critical mole fractions (e.g., 0.33) this heterogeneity appears to be reduced. For example, as shown in Table 2, the reduced χ^2 value of monoexponential fit for $X_{PE} = 0.33$ is significantly lower than that for $X_{PE} = 0.29$ or 0.37. This behavior was observed consistently at most critical compositions. Furthermore, the values of mole fraction of the short-lifetime component (Figs. 4 B and 9 B) appear to reach local maxima near some of the predicted critical mole fractions. These observations indicate that DHE generally senses a more homogeneous environment

in the putative superlattice domains than in the random ones, as predicted by theory (Sugar et al., 1994).

Recently, the formation of DHE transbilayer dimers in lipid membranes has been suggested (Loura and Prieto, 1997). It was proposed that DHE dimer formation increases with the DHE mole fraction and results in a decrease in steady-state anisotropy (Loura and Prieto, 1997). The formation of DHE dimers might offer an alternative explanation of the anisotropy dips as observed in this study. However, using a much smaller amount of DHE (0.2 mol%), we also observed an anisotropy dip near the major critical mole fraction at $X_{PE} = 0.33$ (result not shown). This result indicates that DHE dimer formation may not be the key mechanism explaining the anisotropy dips. However, further studies are needed to determine the role of dimer formation of DHE in PE/PC bilayers.

In conclusion, this fluorescence study provides further evidence that a headgroup superlattice domain can exist in a PE/PC bilayer, as predicted by the headgroup superlattice model. In addition, the observed modulations in the various fluorescence parameters suggest that the existence of the putative superlattice domains may affect the water quenching and rotational motion of membrane sterols in fluid membranes. The annealing study further indicated that several putative superlattice domains are stable or at least metastable for several days at the temperature of measurements.

REFERENCES

Bar, L. K., P. L.-G. Chong, Y. Barenholz, and T. E. Thompson. 1989. Spontaneous transfer between phospholipid bilayers of dehydroergosterol, a fluorescent cholesterol analog. *Biochim. Biophys. Acta.* 983:109–112.

Cheng, K. H., M. Ruonala, J. A. Virtanen, and P. Somerharju. 1997. Evidence for superlattice arrangements in fluid phosphatidylcholine/phosphatidylethanolamine bilayers. *Biophys. J.* 73:1967–1976.

Chong, P. L.-G. 1994. Evidence for regular distribution of sterols in liquid crystalline phosphatidylcholine bilayers. *Proc. Natl. Acad. Sci. USA.* 91:10069–10073.

Chong, P. L.-G., and T. E. Thompson. 1986. Depolarization of dehydroergosterol in phospholipid bilayers. *Biochim. Biophys. Acta.* 863:53–62.

Kao, Y. L., P. L.-G. Chong, and C.-H. Huang. 1990. Time-resolved fluorometric and differential scanning calorimetric investigation of dehydroergosterol in 1-stearoyl-2-caprylphosphatidylcholine bilayers. *Biochemistry.* 29:1315–1322.

Liu, F., I. P. Sugar, and L.-G. Chong. 1997. Cholesterol and ergosterol superlattices in three-component liquid crystalline lipid bilayers as revealed by dehydroergosterol fluorescence. *Biophys. J.* 72:2243–2254.

Loura, L. M. S., and M. Prieto. 1997. Dehydroergosterol structural organization in aqueous medium and model system of membranes. *Biophys. J.* 72:2226–2236.

Parasassi, T., A. M. Giusti, M. Raimondi, and E. Gratton. 1995. Abrupt modifications of phospholipid bilayer properties at critical cholesterol concentrations. *Biophys. J.* 68:1895–1902.

Perrin, F. 1936. Mouvement brownien d'un ellipsoide. II. Rotation libre et dipolarisation des florescences. Transaction et diffusion de molecules ellipsoidoles. *J. Phys. Radium.* 71:1–44.

Schroeder, F. 1984. Fluorescent sterols: probe molecules of membrane structure and function. *Prog. Lipid Res.* 23:97–113.

Schroeder, F., Y. Barenholz, E. Gratton, and T. E. Thompson. 1987. A

fluorescence study of dehydroergosterol in phosphatidylcholine bilayer vesicles. *Biochemistry.* 26:2441–2448.

Somerharju, P., J. A. Virtanen, and K. H. Cheng. 1999. Lateral organisation of membrane lipids. The superlattice view. *Biochim. Biophys. Acta.* 1440:32–48.

Spencer, R. D., and G. Weber. 1970. Influence of Brownian rotation and energy transfer upon the measurements of fluorescence lifetime. *J. Chem. Phys.* 52:1654–1663.

Sugar, I. P., D. Tang, and P. L.-G. Chong. 1994. Monte Carlo simulation of lateral distribution of molecules in a two-component lipid membrane.

Effect of long-range repulsive interactions. *J. Phys. Chem.* 98:7201–7210.

Virtanen, J. A., K. H. Cheng, and P. Somerharju. 1998. Phospholipid composition of the mammalian red cell membrane can be rationalized by a superlattice model. *Proc. Natl. Acad. Sci. USA.* 95:4964–4969.

Virtanen, J. A., M. Ruonala, M. Vauhkonen, and P. Somerharju. 1995. Lateral organization of liquid-crystalline cholesterol-dimyristoyl phosphatidylcholine bilayers. Evidence for domains with hexagonal and center rectangular cholesterol superlattice. *Biochemistry.* 34:11568–11581.